Mon. Not. R. Astron. Soc. **000**, 1–?? (2009) Printed 23 June 2009 (MN LATEX style file v2.2)

Subpulse modulation, moding and nulling of the five-component pulsar B1737+13

Megan M. Force[1] & Joanna M. Rankin[2,1]
[1] *Physics Department, University of Vermont, Burlington, VT 05405*⋆
[2] *Sterrenkundig Instituut 'Anton Pannekoek', University of Amsterdam, NL-1090 GE*

Accepted 2009 month day. Received 2009 month day; in original form 2009 month day

ABSTRACT
Recent Arecibo polarimetric observations of the bright five-component pulsar B1737+13 have facilitated a comprehensive analysis of its pulse-sequence modulation phenomena for the first time. The bright leading component in the star's profile, as well as its other conal components, exhibit a roughly periodic, longitude-stationary modulation with an effective P_3 of about 9 rotation periods. We also find that they show a much slower periodicity at some 91-95 rotation periods. Correlation analyses reiterate these regularities and suggest a modulation pattern moving through the profile negatively. These various properties are largely compatible with a rotating subbeam carousel model having typically 10 'beamlets'. Polar maps are given showing typical subbeam structures that are compatible with the pulsar's somewhat unstable modulation. Geometric analysis finds the central component lagging the center of the traverse of the polarization position angle, suggesting possible effects of retardation and aberration. There remains little overt evidence for the two modes identified earlier, however observed nulls during periods of weak component I emission suggest different behaviors. The pulsar nulls very rarely, but we did identify three pulses in some 5000 that appear to qualify as nulls—presumably pseudonulls or "empty" sightline traverses through the carousel beam system. B1737+13's characteristics are compared with the other well-studied pulsars with double cone/core profiles.

Key words: – pulsars: general, individual (B1737+13)

1 INTRODUCTION

The average pulse profile has often been regarded as the "signature" of a particular pulsar and an important source of information about the emission geometry. While less than a dozen pulsars are known to exhibit five distinct profile components, this group is significant because they display the full complexity of core/cone emission. As is well known (*e.g.*, Rankin 1993; hereafter ETVI), a pulse profile with five components is thought to represent a sightline traverse through two concentric cones and a core beam [see Rankin (1990): fig. 1]. Observations of these stars generally reveal a nearly central sightline traverse of the polarization position angle (hereafter PPA). The hollow emission cones are thought to consist of "carousel" subbeam systems rotating about a star's magnetic axis. The progressive broadening of profiles with wavelength supports this conclusion [*e.g.*, Mitra & Rankin (2002); hereafter ETVII], as does the demonstration of carousel action in a number of pulsars [*e.g.*, B0943+10 (Deshpande & Rankin (1999, 2001; hereafter DR99, DR01), B0834+06 (Rankin & Wright 2007), J1819+1305 (Rankin & Wright 2008)]. These and other recent papers have established multiple connections between the "big three" pulsar modulation phenomena, drifting subpulses, moding and nulling [*e.g.*, Herfindal & Rankin (2007, 2009; hereafter HR0709); Wang *et al.* 2007), and other effects (*e.g.*, "giant pulses" may well be related to them.

Recent single-pulse studies of three five component pulsars, B1237+25, B1857–26 and B0329+54, have provided intriguing new insights into their moding, nulling, subbeam-carousel and core-emission characteristics. In a detailed analysis of several pulse sequences (hereafter PSs) of B1857–26, Mitra & Rankin (2008) found evidence for a subbeam carousel of 20 beamlets, using the methods described in DR01. A 2005 study of PSs of the best known core/double cone pulsar, B1237+25, Srostlik & Rankin

⋆ Megan.Force@uvm.edu; Joanna.Rankin@uvm.edu

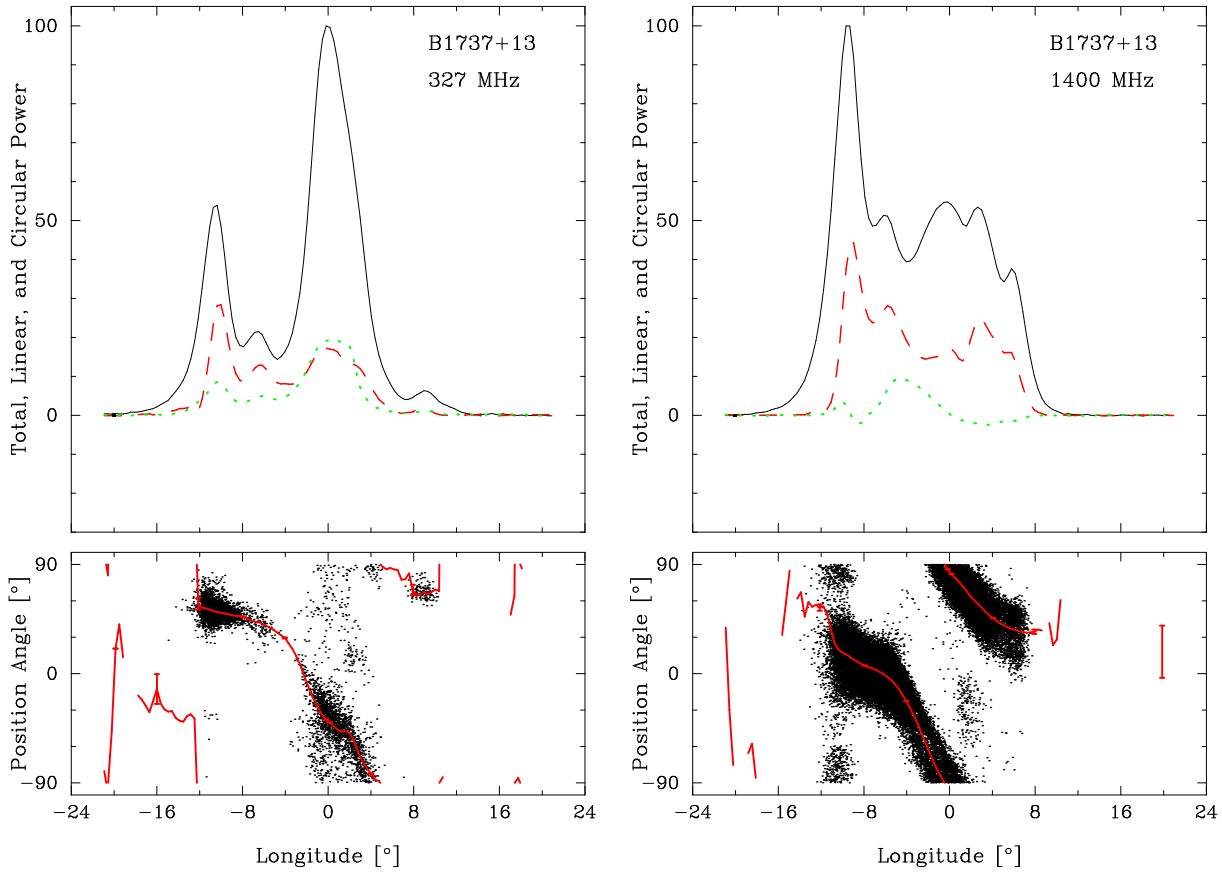

Figure 1. Polarization positon-angle (PPA) histograms for B1737+13 at 327 (**above left**) and 1400 MHz (**above right**) comprised of 2241 and 2055 pulses, respectively. The two panels display the total power (Stokes I), total linear polarization (L [$=\sqrt{Q^2+U^2}$]; dashed red) and circular polarization; dotted green) (upper), and the polarization angle (PPA [$=\tan^{-1}(U/Q)$]) (lower). Individual samples that exceed an appropriate >2 sigma threshold appear as dots with the average PPA (red curve) overplotted. The PPAs are approximately absolute (see text). The small box at the left of the upper panel gives the resolution and a deflection corresponding to three off-pulse noise standard deviations. The histogram of peak pulse intensity (**lower right**) at 1400 MHz corresponds to the profile at the upper right. The star's five components are clearly discernible at this frequency, although at meter wavelengths components III and IV become conflated or even merged as in the 327-MHz profile.

Table 1. Observational parameters.

Frequency (MHz)	Bandwidth (MHz)	Date m/d/yr	$\Delta\varphi$ (°)	Length (pulses)
1400	300	03/12/08	0.11	2055
1425	100	04/10/03	0.23	1022
327	25	01/06/05	0.23	2241

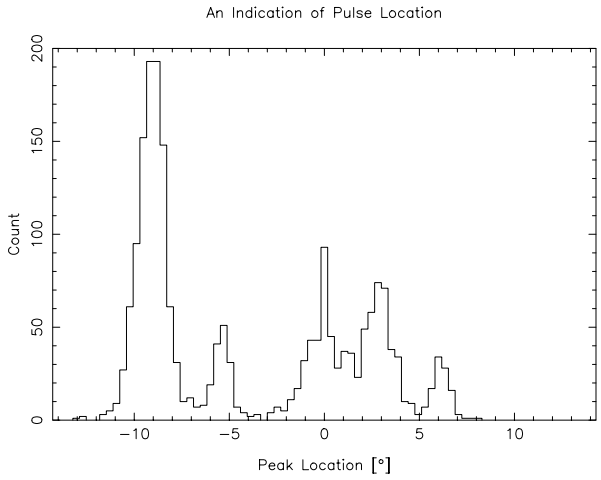

(hereafter SR05) found a previously unknown emission behaviour, intermediate between the pulsar's well known normal and abnormal modes (Backer 1970). This "flare normal" mode is characterized by bursts of activity in the pulsar's core component. In preliminary results, Maan & Deshpande found a likely tertiary period of ∼26.62 stellar-rotation periods (hereafter P_1) for B1237+25. The discovery that many pulsars exhibit periodic nulls that appear to be carousel related [Herfindal & Rankin (2007, 2009)], that drift effects are seen in a large proportion of all pulsars [Weltevrede *et al.* (2006, 2007)], and that mode-changing and nulling are closely connected (Wang *et al.* 2007) raise further intriguing questions about double cone pulsars. Finally, Mitra *et al.*'s (2007) investiga-

tion of pulsar B0329+54's polarized core emission has revealed intensity-dependent aberration/retardation (hereafter A/R) effects apparently reflecting the primary accelerating or height-dependent amplification processes in this star.

These recent results prompted our renewed interest in pulsar B1737+13—the second brightest member of the core/double cone-species within the Arecibo sky—which had received no detailed study in many years. Hankins & Rickett (1986) first clearly delineated the star's five components, distinguishing its components III and IV through their distinct spectra. Deich (1986) discovered the star's roughly 10 rotation-period modulation, seen primarily in comp. I. Early profile polarization measurements (Rankin, Stinebring, & Weisberg 1988) confirmed the expected steep PPA traverse and sense-reversing circular polarization associated with the central component III. More recent profile polarimetry over a broad band (Gould & Lyne 1998; Hankins & Rankin 2009) clearly shows that the core component exhibits a steeper spectrum as is usual, evolving from relative weakness at high frequencies to dominating the profile at long wavelengths.

The most thorough published study of B1737+13 was carried out more than 20 years ago (Rankin, Wolszczan, & Stinebring 1988; hereafter RWS), but from a contemporary perspective it still leaves most questions unaddressed. This effort was based on 1400-MHz observations, both PSs and partial profiles, finding first that the star exhibited two distinct modes and second that a strong periodicity was associated with its leading component. Again, as expected for a central sightline geometry, this 11–14-P_1 periodicity is associated with the strengthening and weakening of its first component—that is, stationary amplitude modulation—but paradoxically they found no discernable periodic modulation associated with components II-IV. RWS found that the above modulation was among the characteristics of the pulsar's "normal" mode of emission, occurring some 85-90% of the time. They also identified an "abnormal" mode, characterized by the prolonged absence of strong component I emission, within the remaining 10% of the PSs. Unlike for B1237+25 and B0329+54 above, they found little difference between the average polarization characteristics of the two modes (see their fig. 5). Interestingly, RWS employed a quasi-two-dimensional cross-correlation function (CCF) to identify a strong correlation between comps. I and V and between components II, III and IV.

In this study we revisit this pulsar using the new methods of investigation employed in DR01 and SR05. In §2 we discuss our observations, and in §3 we discuss the geometry of the pulsar's emission. §4 is dedicated to analysis of the core component, and in §5 we discuss the pulse sequences of B1737+13, including nulling and moding phenomena and the observed low-frequency feature. In §6 we summarize our results.

2 OBSERVATIONS

The observations were carried out using the 305-meter Arecibo Telescope in Puerto Rico. All of the observations used the upgraded instrument with its Grego-

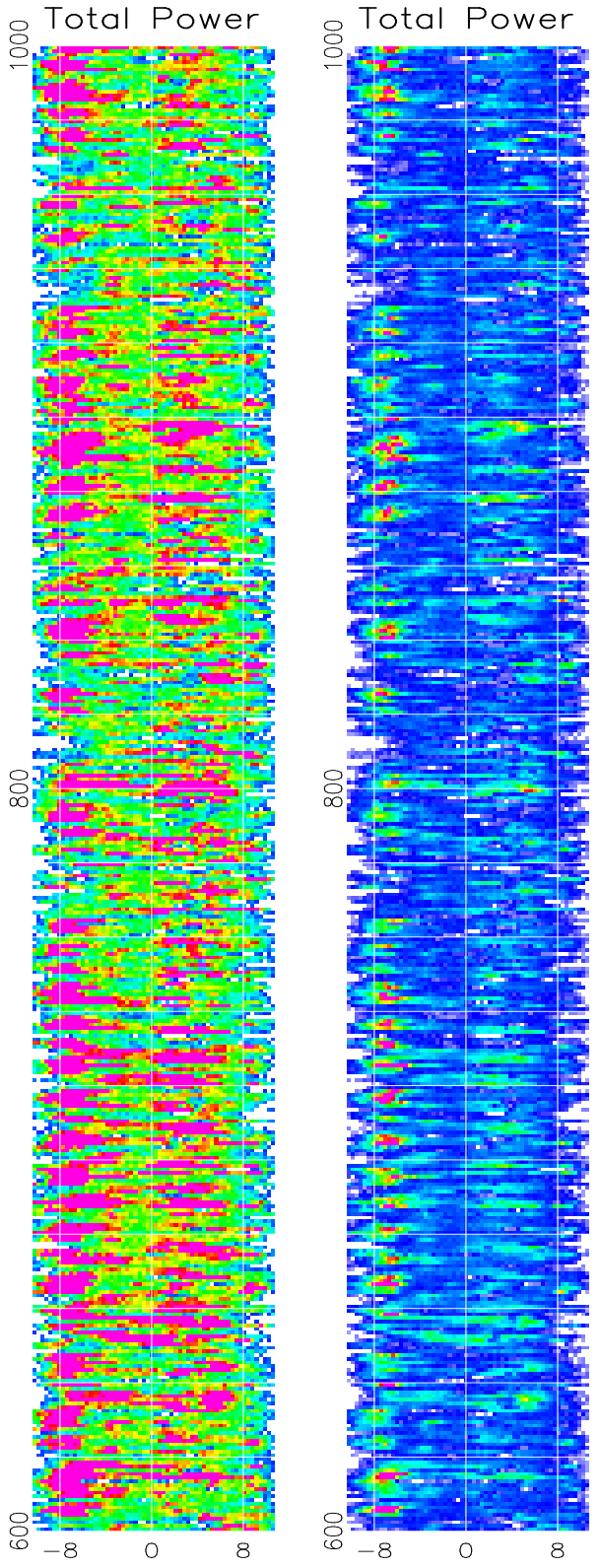

Figure 2. Stokes parameter I is shown for a 400-pulse, L-band sequence using a highly saturated low-intensity (left) and little saturated high-intensity (right) scale according to the same color bar as in Fig. 3. Some tendency of periodic fluctuation in comp. I is apparent, as is the so-called abnormal mode, marked primarily by a lack of strong emission in this component. The low-intensity display reveals a corresponding normal-mode periodicity in comps. II-IV. The longitude origin here is shifted relative to Fig. 1 so that two cones are symmetric about longitude zero; note that this causes the core component (III) here to lag the center of the profile.

Table 2. Aberration/Retardation Analysis Results for B1737+13

Freq/ Cone	ϕ_l^i (deg)	ϕ_t^i (deg)	ν^i (deg)	Γ^i (deg)	r_{em}^i (km)	s_L^i
1400/II	-9.10 ± 0.10	6.19 ± 0.10	-1.46 ± 0.07	5.45 ± 0.06	487 ± 24	0.56 ± 0.01
327/II	-11.50 ± 0.25	8.50 ± 0.25	-1.50 ± 0.18	6.94 ± 0.16	502 ± 59	0.71 ± 0.04
115.5/II	-13.30 ± 0.50	10.50 ± 0.50	-1.40 ± 0.35	8.17 ± 0.32	468 ± 118	0.86 ± 0.11
1400/I	-5.52 ± 0.20	2.85 ± 0.20	-1.34 ± 0.14	3.38 ± 0.11	447 ± 47	0.36 ± 0.02
327/I	-6.79 ± 0.30	3.50 ± 0.40	-1.65 ± 0.25	3.93 ± 0.21	550 ± 84	0.38 ± 0.03

rian feed system, 327 (P band) or 1100-1600 (L band) MHz receiver, and Wideband Arecibo Pulsar Processor (WAPP[1]). The ACFs and CCFs of the channel voltages produced by receivers connected to orthogonal linearly (circularly at P band, after 2004 October 11) polarized feeds were 3-level sampled. Upon Fourier transforming, sufficient channels were synthesized across a 25/100-MHz passbands at P/L band, respectfully, to reduce the dispersion smearing time to about that of the milliperiod sampling interval. The March 2008 observation has three bands combined to give 300 MHz bandwidth. Each of the Stokes parameters was corrected for interstellar Faraday rotation, various instrumental polarization effects, and dispersion. The interstellar and ionospheric contributions to the rotation measure (hereafter RM) were separately determined for each observation (Rankin & Weisberg 2009), and these values used to rotate the PPAs to infinite frequency; therefore the PPAs are approximately absolute. The date, resolution, and the length of the observations are listed in Table 1.

3 GEOMETRY

Figure 1 displays the five-component average profile of B1737+13 at 327 and 1400 MHz. At the lower frequency, the central (putative core) component of this 803-ms ($=P_1$) pulsar dominates the profile and appears to merge with comp. IV. In both cases we see a steep traverse of the PPA near the center of the profile representing some –20°/°. The analysis in ETVI used this value and the profile dimensions to estimate the magnetic latitude angle α and sightline impact angle β as 41 and 1.9/degr—such that β/ρ (where ρ is the outside half-power point of the beam) is 0.40 and 0.28 for the inner and outer cones, respectively. The polarization information provides no clear indication of the sign of β—*i.e.*, whether the sightline traverse is poleward or equatorward of the magnetic axis. Similarly, the partially merged nature of the core component makes its width difficult to determine, but this width is compatible with its expected 1-GHz angular size in terms of the polar cap (ETIV) of 4.2° ($=2.45^\circ P_1^{-1/2} \csc\alpha$). The above analysis demonstrates that the conal beam dimensions of B1737+13 are very nearly identical to those of many other pulsars as scaled to the angular size of the polar-cap emission zone. Moreover, Lyne & Manchester's (1988) method of geometric analysis results in just the same α and β values if their less steep PPA value is corrected.

Also intriguing are the separations of the conal component pairs in relation to the various possible markers of the profile center. Both profiles are asymmetric in that the core lags the midpoints of both conal pairs, a situation that is possibly indicative of aberration/retardation (*e.g.*., see Malov & Suleymanova 1998, Gangadhara & Gupta 2001; hereafter G&G). We can then use G&G's method (as corrected by Dyks *et al.* 2004) to estimate the emission heights of the conal emission in relation to that of the core. The analysis is then virtually identical to that carried out for B1237+25 in SR05, table 1 except that here we have little option but to take the peak of the core component as marking the longitude of the magnetic axis. Values are then given in Table 2 corresponding to the asymmetric separations of the leading and trailing components with respect to the core component. At L band, the measurements are based on both of the profile and peak-occurrance histogram in Fig. 1. At P band only the profile was available, and the merged comps. III and IV make estimation of the latter's position difficult; however, careful inspection shows an inflection on the trailing side of the feature which gives good guidance.

The results in Table 2 are generally compatible with other pulsars with double-conal emission. The (two-sigma) estimation errors are significant for all of the values and indicate emission heights of roughly 500 km, just over twice those estimated using the last-open-field-line geometry (*e.g.*, in ET VI). Also, the inner cone emission appears to reflect a more interior annulus of field lines on the polar cap that that of the outer cone. Interestingly, the core appears to lag behind the steepest gradient (or center) point of the PPA traverse in both the P and L-band profiles of Fig 1 (although this point is not easy to fix with any accuracy).

4 CORE COMPONENT

Given the rich and intriguing effects associated with the core emission in such pulsars as B0329+54 (Edwards & Stappers 2004, Mitra *et al.* 2007) and B1237+25 (*e.g.*, Srostlik & Rankin 2005), we have examined the behaviour of B1737+13's core component carefully. Unfortunately, however, our efforts have given little return. We identify

[1] http://www.naic.edu/∼wapp

this "core" mainly by virtue of its position in the center of the profile (*i.e.*, comp. III); it does show a steeper spectrum than the conal components, but it is hardly marked by antisymmetric Stokes V at L band and not at all in the 327-MHz observation. In both observations the core component exhibits evidence of OPM-produced linear depolarization, and a small population of secondary-polarization mode samples can be discerned on the leading and trailing edges of the core feature.

We have also studied the core emission dynamically, but as can be seen in colour-intensity displays of Fig. 2, its intensity varies over a narrow range and often it is difficult to distinguish from comp. IV. In both the P and L-band PSs, we find that the core participates weakly in the roughly 100-$P-1$ modulation seen more prominently in the conal components (see below). Longitude-longitude cross-correlation functions at zero delay (not shown) do confirm that the core fluctuations are largely independent of comp. IV, and others at delays of up to a few periods show little significant correlation with the other components. Finally, we have examined whether the core component exhibits any shift in position with increasing intensity (as does *e.g.*, the core in B0329+54), and none could be clearly discerned. A weak suggestion of such an effect was present, but our PSs provided so few individual pulses with very strong core emission that the S/N in the higher intensity partial profiles was too poor to reliably judge.

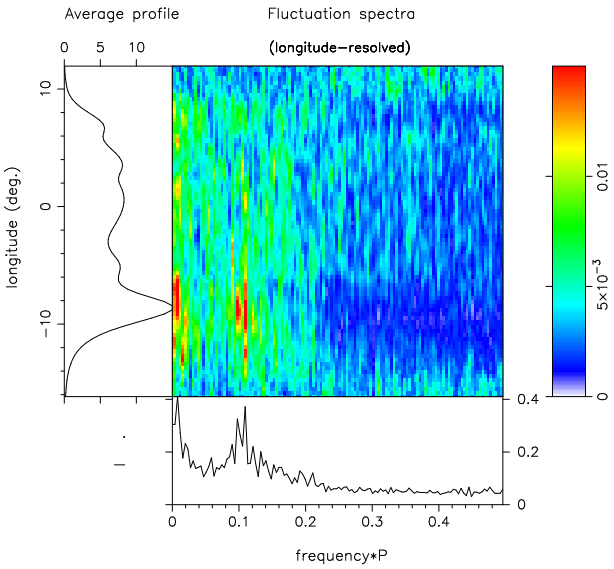

Figure 3. Longitude-resolved fluctuation spectra for the entire B1737+13 PS at 1400 MHz, employing a fast fourier transform (fft) length of 256. The spectra (main panel) are shown relative to the average profile (left panel) and color-intensity coded according to the right-hand bar, with the integral spectrum given in the bottom panel. The broad "hump" of fluctuation power peaking at 8-10 P_1 surely represents RWS's normal-mode modulation. In specific intervals the star's emission is modulated at frequencies around 0.11 c/P_1, corresponding mainly to periodicities of some 9±3 P_1. The surprisingly narrow low frequency feature at roughly 95 P_1, however, was not identified by RWS, and we will consider its significance further below.

5 PULSE-SEQUENCE ANALYSES

5.1 "Modes" and Modulation

In their 1988 paper, RWS discussed B1737+13's emission properties in terms of two modes, "normal" and "abnormal," which differed primarily in the relative strength of comp. I (See their fig. 4). Using an early form of cross-correlation analysis, they found the somewhat unstable normal mode to be characterized by an approximately periodic strengthening of the first component on a cycle of some 11-14 P_1. They then identified PS intervals lacking bright (or periodic) comp.-I emission as representing an abnormal mode. A typical 400-P_1 PS similar to those RWS studied is shown in Figure 2 on two different intensity scales (both coded as in Fig. 3—that is, blue up through green to red and saturating in magenta): one (left) displays the low-intensity emission; whereas the other (right) depicts even the most intense subpulses such that most do not saturate in magenta. While some regularity is discernible, only in the interval between pulses 650 and 750 do we see the bright $\sim 10P_1$, comp.-I modulation characteristic of RWS's "normal mode". Observations of individual pulses suggest that Comp. I often builds up to one or two high intensity pulses before decreasing in intensity each cycle. We do see that the rough periodicities are not confined to comp. I—but often modulate comps. II-IV as well—and that the modulation appears stationary, with no apparent subpulse motion or drift. Bright comp.-V subpulses do seem to accompany bright comp.-I emission as reported by RWS, but we will see below that this correlation is not very strong. Finally, note that this putative interval of RWS's "normal mode" shows no clear boundaries.

Figure 3 gives longitude-resolved fluctuation (hereafter lrf) spectra for the 1400-MHz observation, and a rough, broad feature peaking at some 0.10-0.11 cycles/P_1 corresponds to the normal-mode modulation discussed by RWS. An harmonic resolved fluctuation spectrum (not shown) displays a nearly symmetrical integral spectrum, indicating primarily amplitude (as opposed to phase) modulation—as would be expected for this star's geometry wherein the sightline traverses the emission cones radially. The lrf spectra of short intervals of the PSs show either a broad response or discrete features with P_3 values in the same range between some 8 and 14 P_1.

Our further analyses suggest that the prominence of comp. I varies broadly in different sections of our PSs. On closer inspection we were unable to identify any reliable criterion for assigning specific pulses (or short trains of pulses) to one or the other of RWS's putative modes—a situation very unlike that for other pulsars with several modes. Using fluctuation-spectral methods, we find that intervals of weak comp.-I emission continue to show its characteristic rough periodicities, although at a weaker level of intensity and with less clearly correlated emission in the other comps. Conversely, when comp. I is active, correlated emission is often seen in comps. III-V, suggesting some tendency to periodicity in the core as well

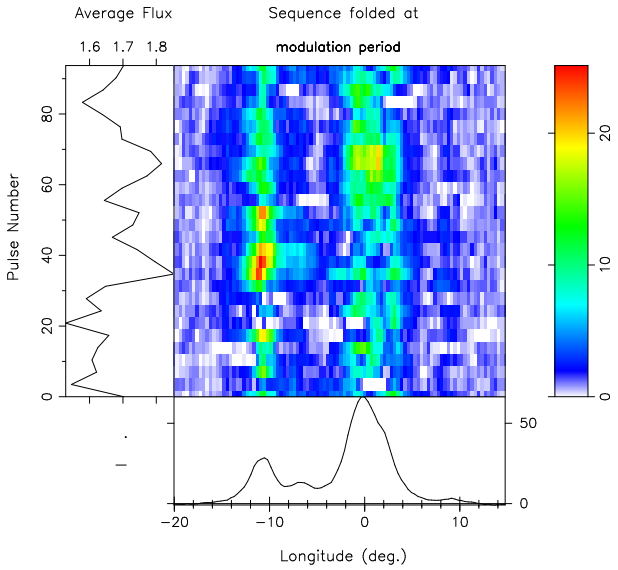

Figure 4. P-band 2241-pulse observations folded at the 93.7-P_1 modulation period. This feature partially modulates all five components, and the "base" (unmodulated power; bottom panel) is removed here to show this clearly. Most obvious in the diagram is the effect on comp. I which exhibits a peak-to-minimum modulation of about 50%. Comps. II and IV (trailing edge) are also comparably modulated, but owing to their weakness, their modulation moves only from blue through cyan to green (Note, the separate comp.IV modulation power at about +4°longitude). Even comp. III shares in this modulation at the 10% level and there is a suggestion of it in comp. V as well.

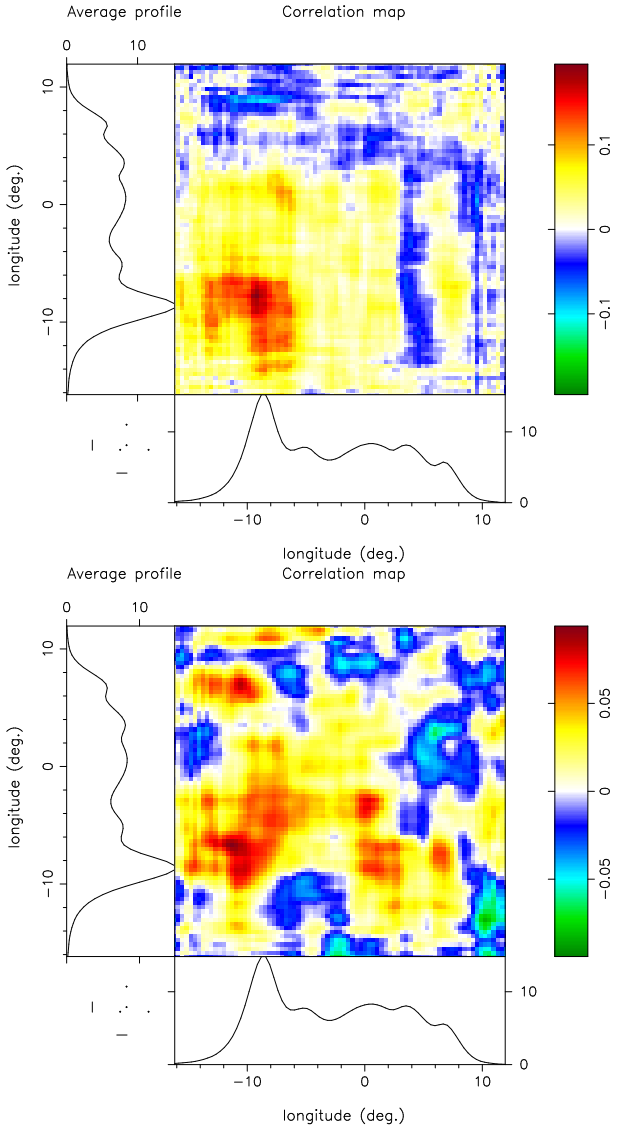

Figure 5. Longitude-longitude correlation plots using delays of 9 periods (top) and 92 periods (bottom) for the 2055-pulse, 1400-MHz PS. Comp. I shows significant correlation with itself in both cases. Note also the correlation between comps. I and V in the lower plot, which is expected in the rotating subbeam carousel model. The three-standard-deviation error in these correlations plots is about 6%. The ordinate is delayed with respect to the abscissa, and the display shows the correlation for positive delay below the diagonal and that for the negative delay about it.

as both cones. Therefore we find little cause to regard RWS's modes as similar to the discrete changes of mode seen in other stars (*e.g.*, B1237+25). We will thus continue to use their terms below as descriptors, but without any implication that they imply the mode-changing phenomenon.

The 327-MHz PS lrf (not shown) is somewhat similar to that above in that it shows both a strong, narrow low frequency feature—here at 93.7±1.0 P_1—as well as a broad "hump" of fluctuation power around 0.1 c/P_1. In order to show the effect of this modulation clearly, we present a folded PS in Figure 4 with the non-fluctuating power ("base") removed. Note, for instance, that the amplitude of comp. I fluctuates over a range from blue to red in the main panel (3 to 25 units) in addition to a base amplitude of roughly 25 units, so is some 50% modulated. Comps. II-IV also show fluctuations at this period and there is a hint that comp. V does as well. This figure very clearly shows the independent behavior of comps. III and IV.

5.2 Low Frequency and "Drift" Modulation Features

The existence of a low frequency modulation feature, having a period of some 93±3 P_1 is depicted in Figs. 3 and 4 above. The feature may also be discerned in the 92-cm 2-D fluctuation spectra of Weltevrede *et al.* (2007). Sections of our PSs at both frequencies as well as their entireties exhibit this feature consistently, and there is a tendency for it to be associated more strongly with "normal-mode" intervals (in RWS terms) which also show a definite comp. I cyclicity. Our long PSs were analyzed in an effort to determine the frequency of this feature as precisely as possible, and although values were encountered in a range between 80 and 120 P_1 in sections of typically 512 pulses, the longer intervals tended to show a narrower low frequency feature. As we have seen (*e.g.*, Fig. 2), the character of the star's overall "normal/abnormal" modulation is unstable and leads to the

broad variations observed in different sections. The two long PSs show a somewhat more stable average behavior in their entirety, and (per the above figures) a value of some 91-95 P_1 obtains. This low frequency fluctuation is also predominantly amplitude modulation as shown by its symmetrical hrf spectrum (not shown).

The longitude-longitude correlation plot at L band in Figure 5 shows a significant correlation between component I and itself at a delay of nine periods (top) and again at 92 periods (bottom) even when averaged over the entire PS. Within the subbeam-carousel model, the first 9-P_1 correlation represents a median value of the drift-modulation period, P_3, and the second one the carousel circulation time $\hat{P}_3$—thus they could be indicative of a carousel having roughly ten "sparks".

Some further indications regarding the structure of the putative carousel are seen in Figure 6, where similar P-band correlation plots are given for delays of both 1 (upper) and 9 (lower) rotation periods. Immediately one is struck by the cross-like form of the correlation maps. These show that at P band most of the correlation is between comps. II and IV. However, at a delay of one period, significant correlation is seen between comps. I (abscissa) and comps. II, IV and V (ordinate)—and note that this correlation is asymmetric in that it occurs in the upper diagonal half of the plot only. This correlation is then between the –1-pulse-delayed comps. (II. IV & V) and the undelayed comp. I, suggesting that the carousel rotates comp. V around to comp. I. Comp. II, by contrast, shows a symmetrical correlation with IV for 1-period delay, suggesting that the geometry is such that carousel rotation brings these two comps. into the sight-line together. The 9-period delay plot (bottom) also emphasizes the inner conal comps. II and IV which are well correlated at an interval corresponding to P_3. The weak correlation between the delayed comp. I and the undelayed comp. V also suggests that the 'beamlet' pattern rotates negatively through the profile.

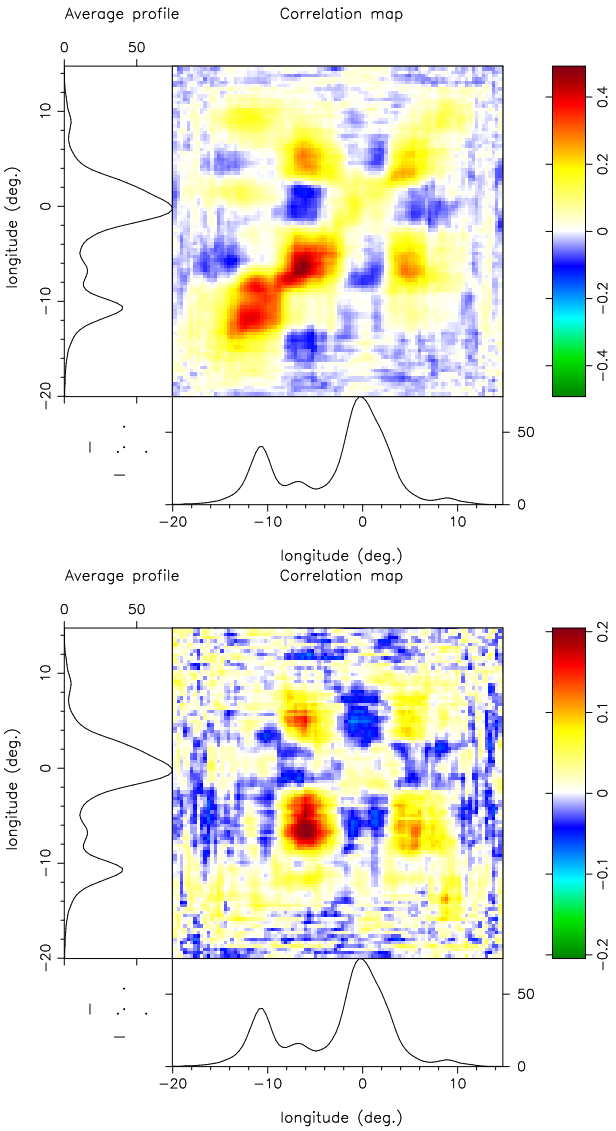

Figure 6. Longitude-longitude correlation maps using delays of 1 period (top) and 9 periods (bottom) for the 327-MHz, 2241 PS. Overall, we see that the inner conal comps. (II and IV) are highly correlated, giving the diagonal "square" of significant correlation. Note, however, the significant and asymmetrical correlation of comp. I with comps. II, IV and V in the upper diagram at –1 period delay, which strongly suggests that the carousel rotates negatively through the emission pattern. The three-standard-deviation error in these correlations plots is about 6%. The ordinate is delayed with respect to the abscissa, and the display shows the correlation for positive delay below the diagonal and that for the negative delay about it.

5.3 Nulling

Much has been learned recently about beamlet carousel systems from the study of "null" pulses, so we were eager to see whether B1737+13 would follow suit. In his 1981 analysis, Backus concluded that B1737+13 displayed a null fraction of less that or equal to 0.02%. Of the three observations considered here, we were able to identify apparent nulls in only one, that at 1425 MHz, and then only in two instances. Both occurred during "abnormal mode" intervals when comp. I was weak or absent. A population of weak pulses, of course, occurs in all three PSs, but the weakest of these are strong enough (and the sensitivity good enough) that they can be distinguished from the baseline noise distribution. Therefore, we tend to believe that nulls do occur in the pulsar but very rarely—and two pulses in some 5000 is indeed 0.02%. Such nulls might not represent cessations of the pulsar's emission but be the pseudonulls identified in other pulsars (*e.g.*, HR0709). We attempted to test this by looking for periodicities in several populations of nulls and weak pulses. No significant periodicities were identified, but we did find that virtually all of the low-intensity pulses were encountered in "abnormal mode" PSs. The contrast between the putative nulls in one observation and only weak pulses in others suggest that the star does in fact display distinct types of behavior.

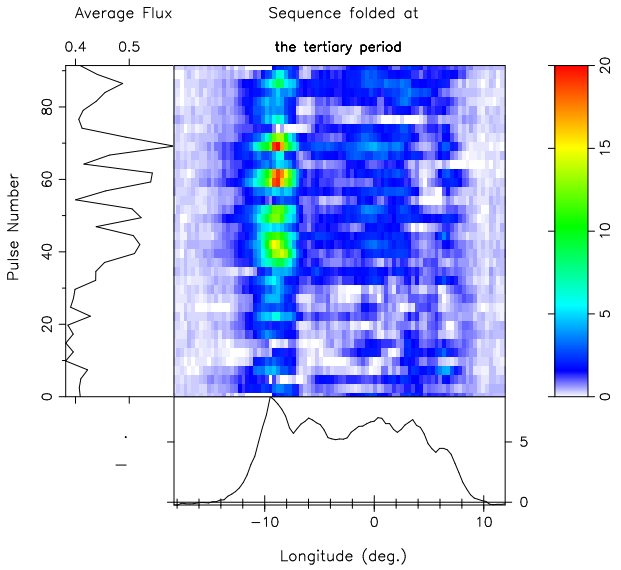

Figure 7. Partial 1400-MHz PS (pulses 1001-2055) folded at 10 times the dominant P_3 feature's period of 9.143 P_1. The unmodulated "base", shown in the bottom panel, has been subtracted from the power in the main panel. The weakish comp. I here is indicative of the star's "abnormal" behavior. The four bright features have a spacing that is compatible with a 10-'beamlet' carousel configuration, and the rough persistence of a half-illuminated carousel over this (and other) intervals of our observations goes far toward explaining why the low frequency feature is so prominent in B1737+13.

5.4 Subbeam-Carousel Structure

We are now in a position to explore whether the various modulation properties identified in the foregoing sections can be produced by a rotating "carousel" of subbeams. The various analyses above have provided consistent evidence for a low frequency modulation of about 93 P_1 that could represent its circulation time $\hat{P}_3$, and the primary subpulse modulation with a P_3 of some 9-13 P_1 could be produced by subbeams passing through the sightline having an appropriate range of angular (and thus time) separations. In order to apply the techniques developed by DR01—in particular their cartographic transformation—it is also important to know the star's basic geometry and the fiducial longitude of the magnetic axis. For the former we can depend on the analysis of ET VI, and for our purposes here we can estimate the latter point to lie in the very center of the profile—that is, equidistant between the leading and trailing conal components. Referring to the measurements in Table 2, we can see that this fiducial point leads the core peak by some 1.5°. Finally, we have seen some evidence above to the effect that the putative carousel pattern rotates negatively through the star's profile; this sense makes little difference for B1737+13 given its dominant amplitude-modulated first component and central sightline traverse, it will be good to utilize this information below.

With the above necessary geometry defined, we can proceed to construct maps of the B1737+13 emission region using the methods of DR01 and, given that the star's modulation is somewhat unstable, it will be important to look at both short intervals characterized by a particular behaviour and longer sections where we may see that particular behaviours persist. Starting with the latter, the second half of the 2055-length L band observation exhibits a strong, narrow modulation feature with a P_3 of 9.143 P_1. Figure 7 shows this interval folded at 10 times this period, and a pattern of four comp.-I 'beamlets' can

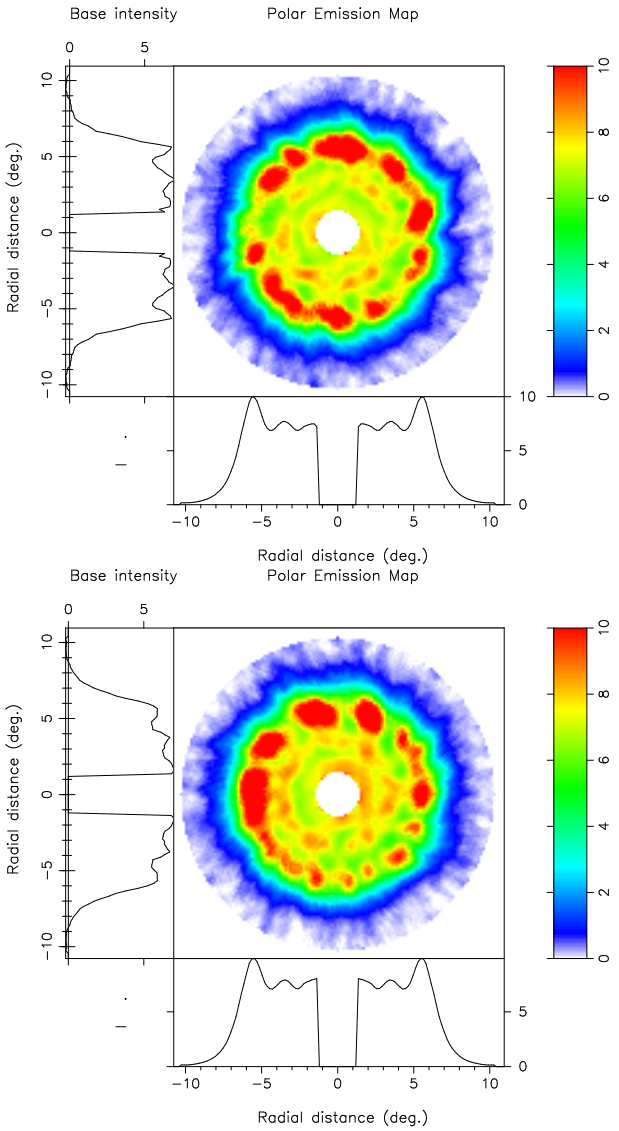

Figure 8. B1737+13 subbeam-carousel "map" pair at 1400 MHz, using a $\hat{P}_3$ identical to the 10×9.143 P_1 folding period of Fig.7. The top and bottom panels display the respective halves of the 2055-pulse observation. The roughly 10-$\hat{P}_3$ average maps show a somewhat disordered 'beamlet' configuration (top) and one having four dominant 'beamlets' with a 10-'beamlet' pattern (bottom). Note that both configurations are irregular enough to generate a low frequency $\hat{P}_3$ fluctuation feature. The "nearer" rotational pole is at the top of the diagrams; and the magnetic axis is in the center of the main panels, such that the sightline traverse passes within 1.9°(=β) of this point along the meridian. These maps are somewhat "overexposed"—that is, satuating in red–in order to show the inner cone region clearly.

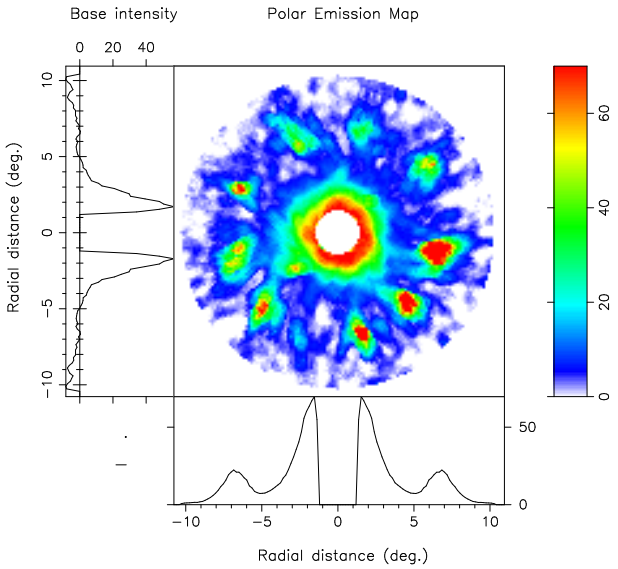

Figure 9. Subbeam carousel "map" of pulsar B1737+13 at 327 MHz. The map is based on a particularly stable pulse sequence (#400-496) at 327 MHz, and shows a carousel configuration of 10 "sparks" with an effective $\hat{P}_3$ value of 93.7 P_1. In general, the pulsar's beam configuration is less regular. The "nearer" rotational pole is at the top of the diagram; and the magnetic axis is in the center of the main panel, such that the sightline traverse passes within 1.9°(=β) of this point along the meridian.

be seen that persist in this average over some 10 circulation times. We take this corrugation as evidence that this folding period does represent the circulation time, and indeed adjacent values tend to exhibit patterns with less fractional amplitude.

The lower display in Figure 8 then shows the corresponding polar map, and it is dominated by four bright 'beamlets' as expected. Note that these four 'beamlets' have magnetic azimuthal separations of about 36°(=360°/10), and they would thus generate a strong "drift"-modulation feature in fluctuation spectra with a P_3 of about 9 P_1—this largely irrespective of the remaining weak 'beamlets' in the outer cone orbit. By contrast, we have also mapped the beginning 1047 pulses in the top display of Fig. 8 in order to emphasize that this somewhat similar pattern produces no strong P_3 feature, but rather a broad "hump" of modulation in the interval from about 0.07-0.12 cycles/P_1. This latter pattern does have some 'beamlets' with a nearly 36°spacing, but most have narrower spacing that would produce higher modulation frequencies.

The colour scale in Fig. 8 is somewhat saturated to show the inner cone region more clearly. While no clear set of 'beamlets' is seen in the inner ring between the core and the outer cone, some ray-like features persist in both maps, but especially in the bottom one. Recall from Fig. 6 that the inner conal comps. II and IV exhibited strong correlation at a delay of 9 P_1, far more than did the outer pair. We do not yet fully understand the relationship or origin of the two conal emission beams in pulsars, but we see evidence here and in other stars that the 'beamlets' in the two cones exhibit a kind of "lock-step" relationship that could explain their similar modulation patterns and mutual correlations.

Finally, Figure 9 gives a polar map for a portion of the 327-MHz observation (pulses 400-496) that overall shows a low frequency feature near 93.7 P_1. In this map we see just 10 'beamlets', though only three are bright and one is almost vanishingly weak. The average radial beamform is shown in the bottom panel and the unmodulated "base"—here interestingly almost entirely core—which has not been subtracted from the map in the central panel. Again, we see little of the inner cone pattern; only one possible "beamlet' can be seen in the map, but the inner cone region is connected by radial "rays" in several cases.

6 SUMMARY AND DISCUSSION

In the foregoing sections we have conducted a full analysis of the pulse-sequence modulation of pulsar B1737+13. A summary of our primary results follows:

- Observations of the pulsar at both P and L bands were studied to detect patterns of emission behavior.
- We confirm that pulsar B1737+13's pulse profile consists of five distinct components, indicating core/double cone emission.
- Periodic fluctuations in components II-IV was observed to correspond to "normal mode" fluctuation in the leading component.
- The core component lags the midpoint of both conal pairs at both P and L bands, and reasonable emission heights are obtained when the positions of the conal component pairs are interpreted as reflecting aberration/retardation.
- A low-frequency modulation feature at some 90-95-P_1 is observed in longitude-resolved fluctuation spectra, and it is found to modulate all five components, with the greatest modulation present in the strong first component.
- Component I is correlated with itself at delays of 9 and 92 periods in our 2055-pulse sequence at 1400 MHz, as expected for a subbeam carousel of some 10 "beamlets".
- The discrete emission features in both the outer and inner conal rings of the polar maps argue that the "beamlet" patterns of both cones rotate with the same period.
- "Complete" nulls were observed to occur very infrequently, with only three such nulls detected in all the observations.

This bright Arecibo pulsar attracted our attention because of its relatively unusual five-component profile, which provides the opportunity to study a double-cone emission system as well as its central core component. B1737+13 is characterized by a nearly-central sightline geometry, though its PA traverse is not as obviously ∼180° as in B1237+25. Like this exemplar of core/double-cone emission, B1737+13's comp. I is both stronger and its modulation features better defined than its comp. V.

Srostlik & Rankin found that B1237+25 exhibits three separate modes(normal, abnormal, and flare-normal), distinguishable often in individual pulses by their respective proportion of primary and secondary polarization mode power. The "normal" and "abnormal" modes identified in B1737+13 by RWS were not confirmed, as no clear boundary could be determined between intervals with and without prominent comp.-I emission. The tendency of the low-frequency feature to be associated with the "normal" mode, as well as the presence of nulls and low-frequency pulses most often in the "abnormal" mode, suggest that a variety of behaviours are present in the emission.

In both B1237+25 and B1737+17, the core component displays a steep spectrum, and is thus observed to be weaker at higher frequencies, while at low frequencies the central component is difficult to isolate due to its near "merging" with the comp. IV in the pulse profile. Whereas B1237+25's core component is strongly active on an episodic basis, B1737+13's core emission is relatively stable. This behaviour is similar to the more regular intensity of the core component in B1857–26.

As with B1237+25 and B1857–26, nulls were found to be of short duration. Unlike these stars, the number of observed nulls in B1737+13 is extremely small, with an estimated null fraction of about 0.02 percent, compared to some 6% in B1237+25 and about 20 percent in B1857–26 (using thresholds of 0.1 and 0.3 $<I>$, respectively. We now know that many observed nulls are in fact "*pseudo*nulls", in which the sightline traverse occasionally "misses" all of the strong "beamlets" in the conal carousel. It is thus probable that the low-intensity pulses and putative nulls observed in the emission of B1737+13 are such pseudonulls.

The observed emission from B1737+13 suggests that a carousel of some 9 or 10 "sparks" or "beamlets" generates the outer cone subpulses of this pulsar. A low-frequency feature of 93±3 periods is identified in the star's lrf spectra, as well as the previously noted unstable drift modulation with a P_3 of 8-14 P_1. A regular periodicity is not only observed in the prominent leading component, but in comps. II-IV as well. Pulse sequences folded at this putative circulation period ($\hat{P}_3$) as well as maps of the star's polar cap confirm that the pulsar's components, particularly comp. I, show a crenelated intensity vs. time structure that largely repeats on a period of some 91-95 P_1. Weak correlation between comps. I and V in longitude-longitude correlation maps further suggests that the modulation sweeps through the profile negatively. In part because of the weakness of comp. V, it is difficult to verify positively that subbeams rotate through the entire profile using correlation maps. Such weaker correlation in the trailing component is also a characteristic of the subbeam carousel observed in B1857–26.

Our analysis of B1737+13's putative core component revealed little of interest, and no clear shift in position with intensity as observed in B0329+54 by Mitra *et al.* (2007). Paradoxically, we found some evidence for correlated emission between the two conal emission beams in the modulation.

The analytical results above have shed further light on a pulsar with an unusual core/double-cone profile, heretofore somewhat unclear for B1737+13 because of its closely spaced comps. III and IV. Overall, we have been able to show that both its profile and modulation characteristics are fully compatible with the model of a core and double-conical beam. Moreover, its pulse modulation seems to reflect a rotating subbeam carousel with a circulation time *P3hat* of some 91-95 P_1. However, this circulation period is greatly longer than the 1.7 P_1 ($=B_{12}/P_1^2$, where B_{12} is the surface magnetic field in units of 10^{12} G) predicted by the Ruderman & Sutherland (1975) model. Indeed, every pulsar with a well measured $\hat{P}_3$ value shows just this behaviour, apparently indicating that the surface field or screened (Gil *et al.* 2009) and/or operate over a larger height range (Harding *et al.* 2002) than this model envisioned.

ACKNOWLEDGMENTS

We are pleased to acknowledge ??? and ??? for their critical readings of the manuscript and Jeffrey Herfindal for assistance with aspects of the analysis. One of us (JMR) thanks the Anton Pannekoek Astronomical Institute of the University of Amsterdam for their generous hospitality and both Netherlands National Science Foundation and ASTRON for their Visitor Grants. Portions of this work were carried out with support from US National Science Foundation Grants AST 99-87654 and 08-07691. Arecibo Observatory is operated by Cornell University under contract to the US NSF. This work used the NASA ADS system.

REFERENCES

Backer, D.C., 1970, *Nature*, 228, 42
Deich, W.T.S., 1986, M.S. Thesis, Cornell University, Ithaca, New York
Deshpande, A. A., & Rankin, J. M., 1999, *Ap.J.*, 524, 1008 (DR99)
Deshpande, A. A., & Rankin, J. M., 2001, *MNRAS*, 322, 438 (DR01)
Dyks, J., Rudak, B., & Harding, A.K. 2004, Ap.J., 607, 939
Edwards, R.T., & Stappers, B.W. 2004, *A&A*, 421, 681 (ES04).
Gangadhara R.T., & Gupta Y. 2001, *Ap.J.*, 555, 31
Gil, J. A., Melikidze, G. I., & Zhang, B. 2009, preprint
Gould, D.M., & Lyne, A.G. 1998, *MNRAS*, 301, 253.
Hankins, T. H., & Rankin, J. M., 2009, *A.J.*, in press
Hankins, T. H., & Rickett, B. J., 1986, *Ap.J.*, 311, 684
Harding, A. K., Muslimov, A. G., & Zhang, B. 2002, *Ap.J.*, 576, 366
Herfindal, J. L., & Rankin, J. M., 2007, *MNRAS*, 380, 430
Herfindal, J. L., & Rankin, J. M., 2009, *MNRAS*, 393, 1391
Lyne, A.G., & Manchester, R.N. 1988, *MNRAS*, 234, 477
Maan, Y., & Deshpande, A. A. 2008, 40 YEARS OF PULSARS: Millisecond Pulsars, Magnetars and More. AIP Conference Proceedings, 983, 103-105.

Malov, I. F., & Suleymanova, S.A. 1998, Astron. Rep. 42, 388
Mitra, D., & Rankin, J. M., 2002, *Ap.J.*, 577, 322 (ETVII)
Mitra, D., Rankin, J. M., & Gupta, Y. 2007, *MNRAS*, 379, 932
Mitra, D., & Rankin, J. M., 2008, *MNRAS*, 385, 606
Srostlik Z., & Rankin J. M., 2005, *MNRAS*, 362, 1121
Rankin, J.M. 1983, *Ap.J.*, 274 333 (ETI)
Rankin, J.M. 1986, *Ap.J.*, 301, 901 (ETIII)
Rankin, J.M. 1990, *Ap.J.*, 352, 247 (ETIV)
Rankin, J.M. 1993, *Ap.J.*, 405, 285 and *Ap.J. Suppl.*, 85, 145 (ETVI)
Rankin, J. M., Stinebring, D. R., & Weisberg, J. M. 1988, *Ap.J. Suppl.*, 324, 1048
Rankin, J. M., & Weisberg, J. M. 2009, in preparation
Rankin, J. M., Wolszczan, A., & Stinebring, D. R., 1988, *Ap.J.*, 324, 1048 (RWS)
Rankin, J. M., & Wright, G.A.E. 2007, *MNRAS*, 379, 507
Rankin, J. M., & Wright, G.A.E. 2008, *MNRAS*, 385, 606
Wang, N., Manchester, R. N., & Johnston, S. 2007, *MNRAS*, 377, 1383
Weltevrede, P., Stappers, B. W., & Edwards, R. T. 2007, *A&A*, 469, 607
Weltevrede, P., Stappers, B. W., & Edwards, R. T. 2006, *A&A*, 445, 243